A Nontetrameric Species Is the Major Soluble Form of Keratin in *Xenopus* Oocytes and Rabbit Reticulocyte Lysates

Jeffrey B. Bachant and Michael W. Klymkowsky

Department of Molecular, Cellular, and Developmental Biology, University of Colorado, Boulder, CO 80309-0347

Abstract. Inside the interphase cell, ~5% of the total intermediate filament protein exists in a soluble form. Past studies using velocity gradient sedimentation (VGS) indicate that soluble intermediate filament protein exists as an ~7 S tetrameric species. While studying intermediate filament assembly dynamics in the *Xenopus* oocyte, we used both VGS and size-exclusion chromatography (SEC) to analyze the soluble form of keratin. Previous studies (Coulombe, P. A., and E. Fuchs. 1990. *J. Cell Biol.* 111:153) report that tetrameric keratins migrate on SEC with an apparent molecular weight of ~150,000; the major soluble form of keratin in the oocyte, in contrast, migrates with an apparent molecular weight of ~750,000. During oocyte maturation, the keratin system disassembles into a soluble form (Klymkowsky, M. W., L. A. Maynell, and C. Nislow. 1991. *J. Cell Biol.* 114:787) and the amount of the 750-kD keratin complex increases dramatically. Immunoprecipitation analysis of soluble keratin from matured oocytes revealed the presence of type I and type II keratins, but no other stoichiometrically associated polypeptides, suggesting that the 750-kD keratin complex is composed solely of keratin. To further study the formation of the 750-kD keratin complex, we used rabbit reticulocyte lysates (RRL). The 750-kD keratin complex was formed in RRLs cotranslating type I and type II *Xenopus* keratins, but not when lysates translated type I or type II keratin RNAs alone. The 750-kD keratin complex could be formed posttranslationally in an ATP-independent manner when type I and type II keratin translation reactions were mixed. Under conditions of prolonged incubation, such as occur during VGS analysis, the 750-kD keratin complex disassembled into a 7 S (by VGS), 150-kD (by SEC) form. In urea denaturation studies, the 7 S/150-kD form could be further disassembled into an 80-kD species that consists of cofractionating dimeric and monomeric keratin. Based on these results, the 750-kD species appears to be a supratetrameric complex of keratins and is the major, soluble form of keratin in both prophase and M-phase oocytes, and RRL reactions.

In interphase cells, >95% of the total intermediate filament protein (IFP)[1] occurs in an insoluble, presumably filamentous form. Pulse-chase studies indicate that newly synthesized IFPs are initially soluble and move into an insoluble, presumably filamentous form with time (see Blikstad and Lazarides, 1983; Issacs et al., 1989). Once assembled, intermediate filaments (IF) are dynamic, with significant assembly/disassembly reactions (see Steinert and Liem, 1990; Skalli and Goldman, 1991; Okabe et al., 1993). Moreover, newly synthesized IFPs incorporate along the length of preexisting IFs (see Coleman and Lazarides, 1992).

The process of IF assembly has been studied extensively in vitro. At concentrations >40–50 μg/ml, nucleation and IFP assembly proceed by a self-assembly pathway that involves several defined oligomeric intermediates (see Heims and Aebi, 1994). IFPs that are competent to coassemble first associate along their central α-helical rod domains in a parallel, in-register manner to form coiled-coil dimers (see Geisler et al., 1992; Fuchs and Weber, 1994). Dimers interact in an antiparallel, staggered fashion to form tetramers. In vitro, an octameric form of IFP has been identified and may represent a discrete assembly intermediate (Ip et al., 1985; Hisanaga and Hirokawa, 1990; Steinert, 1991). It has been proposed that keratin IF elongation under in vitro assembly conditions proceeds by the addition of a variety of small oligomeric species (Coulombe and Fuchs, 1990; Steinert, 1991). In the cell, sucrose velocity gradient sedimentation (VGS) studies indicate that soluble vimentin (Soellner et al., 1985) and keratin

Address all correspondence to Michael W. Klymkowsky, Department of Molecular, Cellular, and Developmental Biology, University of Colorado, Boulder, CO 80309-0347. Tel.: (303) 492-8508. Fax: (303) 492-7744.

Jeffrey B. Bachant's present address is Verna and Marrs McLean Department of Biochemistry, Baylor College of Medicine, Houston, TX 77030.

1. *Abbreviations used in this paper*: IF, intermediate filaments; IFP, IF protein; MRS, modified Ringer's saline; RRL, rabbit reticulocyte lysate; SEC, size-exclusion chromatography; VGS, velocity gradient sedimentation.

(Franke et al., 1987; Chou et al., 1993) exist as a 7 S tetrameric form. Based on these observations, it has been proposed that the tetramer is the basic unit of IF assembly (see Fuchs and Weber, 1994).

The failure to identify "free" (i.e., soluble) IFP monomers or dimers in vivo suggests that tetramer formation occurs rapidly after IFP synthesis. In the case of the keratins, rapid tetramer assembly poses some potential problems. Keratin filaments are heteropolymers composed of equimolar numbers of these type I and II keratin polypeptides (see Fuchs and Weber, 1994). The assembly competent form of keratin appears to be a type I/II heterodimer (Coulombe and Fuchs, 1990; Hatzfeld and Weber, 1990; Steinert, 1990). Type I and II homodimers can form in vitro and can be incorporated into IFs (see Steinert, 1990), but are unable to form an IF on their own. Studies of native keratin filaments, however, reveal that little, if any, homodimeric keratin is present in the cell (Steinert, 1990; Pang et al., 1993). Given that keratin homodimers formed in vitro are relatively stable (see Steinert, 1990), it seems likely that cells possess mechanisms for suppressing the formation and/or accumulation of keratin homodimers.

We have been using the *Xenopus* oocyte as a model system for the study of factors controlling keratin filament assembly and network organization (see Klymkowsky, 1995). When compared to cultured cell systems, the late stage *Xenopus* oocyte displays a number of unique properties. First, it is an immobile cell with a readily detectable pool of soluble keratin (Gall and Karsenti, 1987). Because of its immobility, processes involved in the reorganization of IFs during cell locomotion do not occur. Second, the late stage oocyte is arrested in prophase of the first meiotic nuclear division and is not growing. It is therefore likely that the rates of IFP synthesis and degradation equal one another, a situation that simplifies the study of IF assembly dynamics. Third, the oocyte possesses a compositionally simple keratin-type IF network composed of a single type II keratin and two type I keratins (Franz et al., 1983). Fourth, this keratin filament network is organized in an asymmetric fashion, composed of an extended "geodesic" system of filaments in the vegetal hemisphere of the oocyte, and a fragmented network of filaments in the animal hemisphere (Klymkowsky et al., 1987). There is no evidence for differential posttranslational modification of IFPs in the two hemispheres, suggesting that asymmetrically distributed cytoplasmic factors modulate keratin network organization (see Klymkowsky, 1995). Finally, during meiotic maturation, the keratin network of the oocyte undergoes the most complete disassembly yet described for cytoplasmic IFs; the entire keratin filament system is solubilized and then reassembled into filaments after fertilization (see Klymkowsky et al., 1991; Klymkowsky, 1995). In contrast, localized disassembly of IFs appears to occur primarily in the region of the contractile ring in somatic cells (see Nishizawa et al., 1991).

In this work, we used pulse-chase and biochemical fractionation methods to characterize the assembly dynamics of the *Xenopus* oocyte's keratin filament system. As expected, we find evidence for a rapid exchange between soluble and insoluble forms of keratin. Unexpectedly, size-exclusion chromatography (SEC) indicated that the major soluble form of keratin in both prophase and matured oocytes has an apparent molecular weight of ~750,000, in striking contrast to the expected ~150,000 of keratin tetramers (Coulombe and Fuchs, 1990). A similar 750-kD keratin complex was found in rabbit reticulocyte lysates (RRL) translating both type I and type II *Xenopus* keratin RNAs. Based on its behavior under conditions of partial denaturation, the 750-kD form appears to contain keratin tetramer as part of a larger complex. These results suggest that the 750-kD keratin complex is the predominant intermediate in the assembly of keratin filaments in the *Xenopus* oocyte.

Materials and Methods

Oocyte Culture and RNA Injection

Oocytes were isolated from adult female *Xenopus* following established methods (see Klymkowsky et al., 1987) and cultured in modified Ringer's saline (MRS) supplemented with 50 μg/ml gentamycin. For radiolabeling, oocytes were labeled in 250 mCi/ml [^{35}S]methionine (EXPRE^{35}S^{35}S protein labeling mix, sp act >1,000 Ci/mmol, New England Nuclear, Boston, MA) in MRS. For pulse-chase analysis, labeled oocytes were washed extensively in MRS supplemented with 10 mM L-methionine (Sigma Chemical Co., St. Louis, MO) and then incubated in the same MRS/methionine medium. To induce oocyte maturation, oocytes were treated with 5 μg/ml progesterone for 8–10 h before fractionation. Oocytes were injected with in vitro synthesized RNA as described previously (Dent et al., 1992). Typically, 40–50 nl of RNA were injected into each oocyte at concentrations ranging from 250 to 750 μg/ml. After injection, oocytes were allowed to recover in MRS at 16°C.

Construction of Myc-tagged Keratins and In Vitro RNA Synthesis

Two *Xenopus* keratin cDNAs were used in our studies: XK1 and DG81A. DG81A (provided by T. Sargent, National Institutes of Health) encodes a *Xenopus* type I keratin that appears shortly after the midblastula transition (Jonas et al., 1985); an NIH BLAST system amino acid sequence homology search indicates that DG81A is most similar to the human epidermal type I keratin K14 (not shown). XK1 was isolated from a λgt11 cDNA expression library made from *Xenopus* A6 cell mRNA (see Bachant, 1993). DNA sequencing revealed that XK1 is closely related to the XK1(8) cDNA characterized by Franz and Franke (1986); only a few nucleotides are altered between the two cDNAs. XK1 appears to be most similar to human type II simple epithelial keratin K8.

Myc-tagged forms of the XK1 and DG81 keratins were prepared using PCR as described previously for vimentin (Dent et al., 1992). Amplified DNAs were subcloned into either the RNA synthesis vector pSP64T (Krieg and Melton, 1984) (provided by D. Melton, Harvard University, Cambridge, MA) or into the bacterial expression vector pET3b (Studier et al., 1990) (provided by W. Studier, Brookhaven National Laboratory, Upton, NY). For PCR 1 μg of template DNA was combined with 3 μg of each oligonucleotide primer; 30 cycles of PCR were run using a temperature regime of 1 min at 95°C, 2 min at 50°C, and 5 min at 72°C for each cycle. Sequencing of the final constructs revealed a T → G substitution in the codon for amino acid 498 of XK1 (valine → valine), and T → G substitution in the codon for amino acid 424 of DG81 (valine → glycine). The final sequence of the COOH terminus of the encoded proteins was

"keratin.SRDSTMEQKLISEEDLN.stop"

where the underlined sequence is the myc tag.

Synthetic, capped RNAs were prepared as described previously (see Dent et al., 1992). pET3b plasmids containing the XK1.myc and DG81.myc inserts were transformed into *Escherichia coli* strain BL21(DE3), and the synthesis of myc-tagged keratins was induced by adding 0.4 mM isopropylthio-D-galactoside to cultures grown to approximately mid-log phase (OD_{600} = 0.6–1.0). After ~2–4 h of induction, aliquots of the induced cultures were directly solubilized in SDS-PAGE sample buffer (see Domingo et al., 1992).

Oocyte Fractionation

Soluble and insoluble fractions of oocytes were prepared as described previously (Klymkowsky et al., 1991) with some minor modifications. Oocytes were manually homogenized in SOL buffer (140 mM KCl, 2 mM $MgCl_2$, 5 mM EGTA, 10 mM Na_2HPO_4, 5 mM NaF, 300 mM sucrose, 0.5% Triton X-100, 10 mM Tris HCl, pH 7.5, 10 mM PMSF). Labeled oocytes were homogenized in SOL buffer containing 1 mM L-methionine. After centrifugation (15 min at 13,000 rpm at 4°C), the pellet was resuspended in 1 ml of XEX buffer (1.5 M KCl, 5 mM EGTA, 5 mM NaF, 300 mM sucrose, 0.5% NP40, 10 mM Tris HCl, pH 7.5) and then centrifuged again; the pellet of this centrifugation formed the insoluble fraction. The supernatant of the initial centrifugation was extracted with 0.5 ml 1,1,2-trichlorotrifluoroethane (Aldrich Chemical Co., Milwaukee, WI) to remove yolk and lipid (Gurdon and Wickens, 1983), and the aqueous and freon phases were separated by centrifugation. The upper aqueous phase was taken as the soluble fraction.

Immunoprecipitation

Keratin was immunoprecipitated from the soluble fraction using the mouse anti-type II keratin mAb 1h5 (IgG_1) (Klymkowsky et al., 1987) or, in the case of myc-tagged keratin, the anti-tag mAb 9E10 (IgG_2) (Evans et al., 1985). In control experiments the anti-β-tubulin antibody E7 (IgG_2) (Chu and Klymkowsky, 1989) was used. Protein A–purified antibodies (final concentration, 5 μg/ml) were incubated with the soluble fraction for 1 h at 4°C. Protein A–bearing cell walls of *Staphylococcus aureus* (Immunoprecipitin; Bethesda Research Laboratories, Bethesda, MD) were then added (50 μl of a 10% suspension). After a 30-min incubation at 4°C, immune complexes were isolated by a brief centrifugation. The pellet was washed five times in SOL buffer containing 0.5 M NaCl. A number of other wash buffers, including buffers containing 0.2% SDS and 0.5% NP40, higher salt concentrations and distilled H_2O were tested. None of these reproducibly lowered immunoprecipitation background levels (not shown).

Electrophoresis Conditions and Western Blotting

Proteins were analyzed on 10% SDS-PAGE gels. Bacterially synthesized keratins (see above) and prestained protein molecular weight standards (Sigma Chemical Co.) were used as markers. In most cases, samples for two-dimensional gel analysis were solubilized in 9 M urea, 4% NP40, 2% pH 9–11 ampholines (Sigma Chemical Co.), and 2% β-mercaptoethanol. To examine the denaturation of keratin complexes at different urea concentrations, samples from rabbit reticulocyte translation reactions were diluted into sample buffer such that the final urea concentration was 4, 6, or 8 M. Isoelectric focusing tube gels were prepared and run as described previously (Klymkowsky et al., 1991) using a 1:1 mixture of pH 3–10 and pH 4.5–6 ampholines. In urea denaturation experiments, two-dimensional gel electrophoresis conditions were modified following procedures established by Franke et al. (1983) and Hatzfeld and Franke (1985). The concentration of urea in the tube gel was changed to 4, 6, or 8 M, and the ampholine ratio was changed to 1:2 mixture of pH 3–10 and pH 4–7 ampholines. In reduced urea gels, the best results were obtained by reducing electrophoresis in the first dimension to ~5,000–6,000 V h. For immunoblot analysis, polypeptides were transferred to nitrocellulose, and bound primary antibody was visualized using either peroxidase or alkaline phosphatase–conjugated secondary reagents (Bio-Rad Laboratories, Richmond, CA) (see Dent et al., 1992).

Reticulocyte Lysates Translation Reactions

RRLs were purchased from Promega Biotec, Madison, WI; under our conditions, lysates from other suppliers proved less efficient at translating keratin RNA and in producing the 750-kD keratin complex. Translation reactions were performed according to the manufacturer's specifications for 0.5–1 h at 30°C using capped RNAs transcribed from the pSP6.keratin.myc plasmids (see above). The protease inhibitors PMSF (1–5 mM) and *p*-tosyl-*l*-arginine methyl ester (1 mM) were added to RRL translation reactions. In some experiments, the translation reaction was terminated by the addition of cyclohexamide (100 μg/ml) and RNAse A (0.5 mg/ml). To remove ATP and to prevent further nucleotide triphosphate hydrolysis in the RRL, apyrase (20 U/ml; Sigma Chemical Co.) was added for 5 min at 30°C, and then EDTA (10 mM) was added. ATP levels were measured using a commercially available luciferin/luciferase detection system (Sigma Chemical Co.).

Sucrose Velocity Gradient Sedimentation

Soluble oocyte fractions or translation reactions (~0.5 ml final volume) were analyzed on 10-ml 5–30% or 5–20% (wt/vol) linear sucrose velocity gradients. Gradients were prepared from solutions of 140 mM KCl, 2 mM $MgCl_2$, 5 mM EGTA, 10 mM Tris base, pH 7.5, or 140 mM NaCl, 25 mM Tris base, pH 8.0, containing the desired concentration of sucrose. Gradients were centrifuged in a rotor (model SW41; Beckman Instruments, Inc., Fullerton, CA) at 29,000 rpm for 15–18 h at 5°C. Fractions were collected and analyzed either by precipitation with ice-cold 10% TCA, immunoprecipitation with 1h5 or 9E10, or by scintillation counting. Thyroglobulin (19 S), catalase (11 S), immunoglobulin (7 S), and cytochrome C (2 S) were used as sedimentation velocity markers (Smith, 1970).

Gel Filtration Chromatography

For gel filtration chromatography, Superose® 6 and 12 fast performance liquid chromotography (FPLC) columns (Pharmacia Fine Chemicals, Piscataway, NJ) were used. In experiments examining the form of soluble keratin under physiological conditions, columns were run at 4°C in a buffer of 200 mM NaCl, 100 mM K_2HPO_4/KH_2PO_4, pH 7.5 (Yaffe et al., 1992); Superose® 6 columns were run at a flow rate of 0.5 ml/min, and Superose® 12 columns were run at a flow rate of 0.3 ml/min. In urea denaturation experiments, Superose® 12 columns were run at 4°C at a flow rate of 0.3 ml/min in a buffer of 50 mM Tris 7.5, 10 mM β-mercaptoethanol, 10 mM PMSF containing ultrapure urea (Fisher Scientific, Pittsburgh, PA) at concentrations of 2, 4, 6, or 8 M. Before analysis of urea-denatured samples, columns were equilibrated with greater than two column volumes. All buffer solutions were filtered (0.2-μm pore size) before use. Before chromatography, all samples except those denatured in urea were spun in a microfuge for 10 min at 4°C. In urea denaturation experiments, urea was added directly to the sample to achieve the desired final concentration. Unincorporated label was removed from RRL translation reactions using spin columns (Sephadex® G-50; Sigma Chemical Co.) before the lysates were applied to the Superose® columns. Fractions (0.5 ml) were collected and analyzed by scintillation counting, immunoprecipitation, TCA precipitation, or immunoblotting. Columns were calibrated using thyroglobulin (670 kD), catalase (232 kD), immunoglobulin (150 kD), β-galactosidase (119 kD), BSA (66 kD), and lysozyme (14.5 kD) as size markers. For RRL translation reactions, the elution of residual charged tRNA (40 kD) was also used as a molecular weight standard (Yaffe et al., 1992). Void volumes were determined using blue dextran (mol wt ~2×10^6; Sigma Chemical Co.); the included volume was determined using phenol red (354 D).

Kinetic Modeling

The approach to kinetic modeling used here is similar to that used by Isaacs et al. (1989). It is assumed that keratin filaments assemble from a soluble intermediate at a rate proportional to the concentration of soluble keratin and that keratin assembly is irreversible over the course of the experiment. It is also assumed that neither the rate of keratin synthesis nor the number of assembly sites limits assembly. Under these conditions, the chase of soluble keratin into the insoluble fraction should exhibit first order kinetics and have an apparent half-life ($t_{1/2}$) determined by the equation:

$$N_t/N_o = e^{-kt} \quad (1)$$

where N_o = cpm soluble keratin at the beginning of the chase, N_t = cpm soluble keratin after a chase of t min, and k is a first order rate constant (1/min). At $t_{1/2}$, $N/N_o = 0.5$ and thus, $t_{1/2} = 0.693/k$. Rearranging equation 1 into a linear form yields:

$$\log N_t = (k/2.3)\, t + \log N_o \quad (2)$$

Plotting the log of soluble keratin with chase time should yield a straight line with a slope (m):

$$m = -0.693/(2.3 \times t_{1/2}) \quad (3)$$

Given the assumptions described above, it is also possible to calculate a predicted $t_{1/2}$ by following the distribution of keratin between soluble and insoluble forms during a labeling period using Eq. 4 (Caplan et al., 1986):

$$F_a(t) = 1 - [(1 - 0.5^{t/t_{1/2}})\,(t_{1/2})/\ln 2 \times t] \quad (4)$$

where $F_a(t)$ is the fraction of keratin assembled after a continuous pulse of t min. Slopes and linear functions used for half-life calculations were derived from pulse-chase data using the linear regression program included in the graphing application from Cricket Software (Malvern, PA).

Results

The keratin filament system of the *Xenopus* oocyte is composed of a 56-kD K8-like type II keratin and two type I keratins of 46 and 42 kD (see Klymkowsky, 1995). 1–10% of the total keratin has been reported to occur in a soluble form (Gall and Karsenti, 1987) that presumably represents the pool of soluble assembly intermediates. To analyze the distribution of keratin between soluble and insoluble forms, oocytes were fractionated, and the keratin in the soluble compartment was immunoprecipitated with the anti–type II keratin antibody 1h5. Two-dimensional gel analysis followed by Western blotting with the 1h5 antibody of soluble and insoluble fractions was consistent with the previous estimates of oocyte keratin distribution; ~95% of total keratin was found in the insoluble fraction (Figs. 1 *A* and 2). Both soluble and insoluble forms of keratin displayed similar levels of posttranslational modification (Fig. 1 *A*; see Gall and Karsenti, 1987; Chou et al., 1993). The distribution of keratin between soluble and insoluble forms did not change appreciably over a 24-h period in culture (not shown). In addition, the percentage of keratin in the insoluble fraction was not significantly altered by re-extracting the insoluble pellet with the original homogenization buffer or buffers that have been reported to solubilize other IFs (see Chou et al., 1993), including a low salt buffer (10 mM Tris 8.0), a high salt buffer (1.5 M KCl), or buffers containing the detergents NP40 (0.5%) or cetyltrimethylammonium bromide (1%) in place of Triton X-100 (not shown). Immunoprecipitation of soluble keratin appeared to be due to a specific interaction between keratin and the 1h5 antibody; in the absence of the 1h5 antibody, or in the presence of a nonkeratin antibody, the type II keratin was not precipitated (Fig. 1 *B*). In addition to the intact keratin polypeptide, a smaller 1h5-reactive polypeptide was frequently observed in 1h5 immunoprecipitates (Fig. 1 *B*). This polypeptide appears to be a proteolytic fragment of the intact polypeptide; a similar processing event is seen when exogenous keratin is expressed in the oocyte or in reticulocyte lysates (see below).

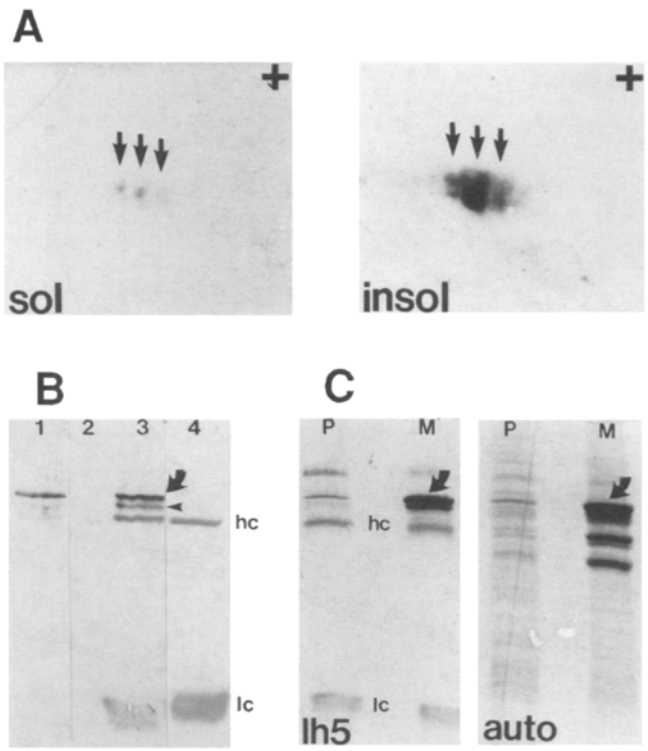

Figure 1. Endogenous keratins in the *Xenopus* oocyte. (*A*) Analysis of soluble (*sol*) and insoluble (*insol*) keratin by two-dimensional gel electrophoresis/Western blotting using the 1h5 antikeratin antibody revealed a similar pattern of isoelectric variants (*arrows*; +, acidic end of the IEF gel). (*B*) Soluble keratin was immunoprecipitated from groups of 20 oocytes using 1h5 (lane *3*). Immunoblotting of the immunoprecipitates with 1h5 revealed a 1h5-reactive polypeptide (*arrow*) that comigrated with bacterially synthesized XK1.myc polypeptide; the smaller 1h5-reactive polypeptide (*arrowhead*) appears to be a proteolytic fragment of the XK1 polypeptide. No 1h5-reactive polypeptides were precipitated by the anti–β-tubulin antibody E7 (lane *4*) or in the absence of primary antibody (lane *2*). (*C*) Immunoprecipitation of soluble keratin from 20 prophase (*P*) or progesterone-matured (*M*) oocytes revealed that the amount of soluble XK1 polypeptide increased during maturation (*arrows*). Autoradiography of the Western blot (*auto*) revealed that two non–1h5-reactive coprecipitated polypeptides also increased in abundance; these are likely to be the type I keratins of the oocyte. (*hc* and *lc*, antibody heavy and light chains).

To examine the association of other proteins with type II keratin, oocytes were labeled with [^{35}S]methionine, and the polypeptides that coimmunoprecipitated with soluble keratin were examined. With the relatively small amount of soluble keratin present in prophase oocytes, the 1h5-reactive type II keratin was the predominant radiolabeled polypeptide observed (Fig. 1 *C*). To increase the amount of soluble keratin, oocytes were matured with progesterone; under these conditions, the entire keratin filament system disassembles into soluble oligomers (Klymkowsky et al., 1991). Both the soluble 1h5-reactive type II keratin and two non–1h5-reactive polypeptides increased in 1h5 immunoprecipitates after maturation (Fig. 1 *C*). These two polypeptides had molecular weights of ~46,000 and 42,000 and are likely to be the two type I keratins of the oocyte, presumably in a complex with the type II keratin (Franz et al., 1983).

Relationship between Soluble and Insoluble Keratin

To examine the assembly of newly synthesized keratins, oocytes were labeled in [^{35}S]methionine for varying lengths of time, fractionated, and the amount of radioactivity associated with soluble vs. insoluble type II keratin was quantitated. The rate of incorporation of radioactivity into both soluble and insoluble keratin was constant over a 24-h period; at each time point, 90–95% of the newly synthesized keratin was present in the insoluble form (Fig. 2, *A–C*). Keratins are a minor biosynthetic component of the oocyte and are synthesized at a relatively low overall rate. We therefore examined the effects of increasing the rate of keratin synthesis by injecting oocytes with RNAs encoding the *Xenopus* type I keratin DG81A and the *Xenopus* type II keratin XK1. We chose to use both type I and type II keratins to minimize complications that might arise from the unbalanced synthesis of unpaired keratins. Both keratins were tagged at their COOH termini with the myc epitope (MEQKLISEEDLN.stop) to facilitate the separa-

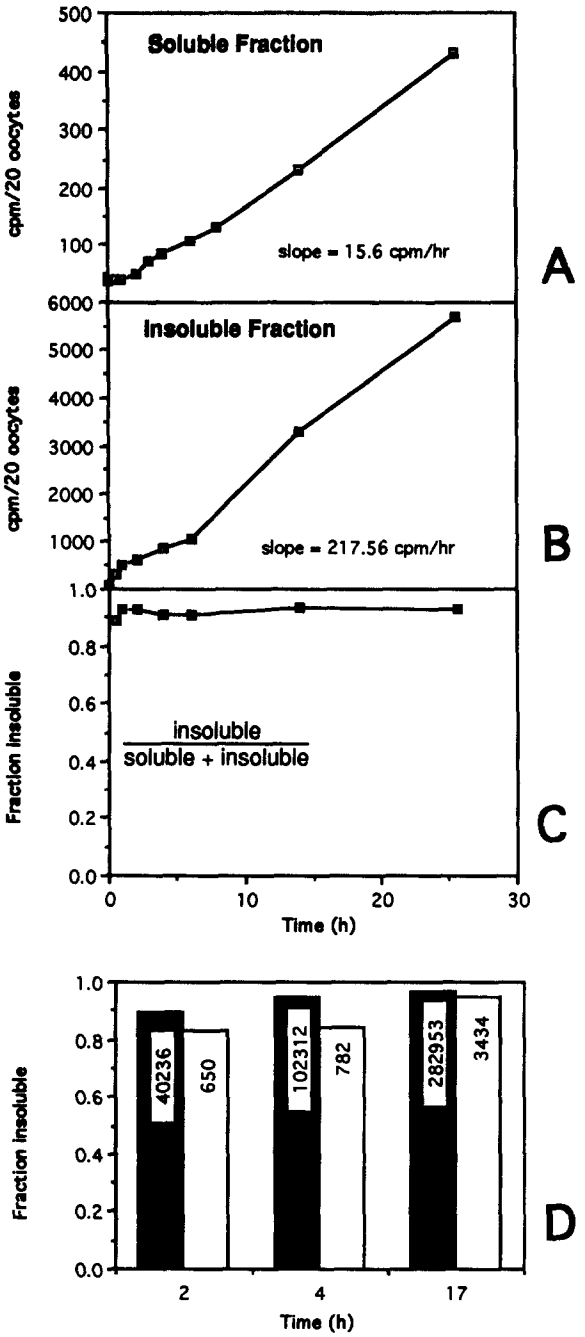

Figure 2. Fractionation of endogenous and exogenous keratins in the oocyte. The soluble fraction of [^{35}S]methionine-labeled oocytes was immunoprecipitated with 1h5, while insoluble fractions were analyzed by two-dimensional gel electrophoresis. The distribution of type II keratin between the two fractions was quantitated by measuring the radioactivity associated with 1h5-reactive polypeptides. In both soluble (*A*) and insoluble (*B*) fractions, radioactive keratin accumulated in a linear fashion with time. At each time point, 90–95% of the newly synthesized keratin was found in the insoluble fraction (*C*). Similar results were seen when oocytes were injected with RNAs encoding myc-tagged forms of the type I keratin DG81 and the type II keratin XK1 (*D*). At 2, 4, and 17 h after addition of the label, the fraction of the 9E10- (anti-myc) reactive exogenous XK1.myc keratin (*solid bars*) present in the insoluble fraction was determined and compared to the fraction of endogenous 1h5-reactive type II keratin present in the insoluble fraction (*open bars*) of uninjected oocytes of the same batch. Synthesis of exogenous keratins greatly increased the overall rate of keratin synthesis (numbers in boxes, cpm associated with insoluble XK1.myc keratin).

tion of either endogenous or exogenous keratins. Previously, we have shown that this tagging sequence at a COOH-terminal location does not affect the assembly properties of *Xenopus* vimentin or desmin (Dent et al., 1992; Cary and Klymkowsky, 1994). When injected into cultured amphibian A6 cells or into the *Xenopus* oocyte, these myc-tagged keratins coassemble with the endogenous keratin filament network (see Bachant, 1993). In three separate batches of RNA-injected oocytes, exogenous myc-tagged keratins partitioned into both the soluble and insoluble fractions and led to an increase in the overall rate of keratin synthesis ranging between 10–90-fold over that seen in uninjected oocytes (e.g., see Fig. 2 *D*). Under these conditions the distribution of newly synthesized exogenous keratin between the soluble and insoluble fractions was similar to the distribution observed for endogenous keratin in uninjected oocytes of the same batch, i.e., ~90% of the total exogenous keratin was found in the insoluble fraction at all time points examined (Fig. 2 *D*). We therefore conclude that this "unnatural" K8/K14 keratin pair behaves essentially the same as the K8/K18–K8/K19 keratin pairs nomally present in the oocyte.

If keratin polypeptides assemble irreversibly into keratin filaments, the distribution of keratin between soluble and insoluble fractions (Fig. 2) can be used to calculate the half-life of soluble keratin in the oocyte in pulse-chase experiments (Eq. 4 from *Materials and Methods*); according to this calculation, soluble keratin should display a half-life of ~30 min. To test this prediction, oocytes were labeled with [^{35}S]methionine for 4 h, washed, and then chased with 10 mM unlabeled methionine for 20 h. After a period of several hours, during which the large methionine pool of the oocyte equilibrates with cold methionine (see Wallace and Hollinger, 1979), incorporation of radioactivity into both soluble keratin and total oocyte protein was blocked (Fig. 3, *A–C*). The half-life of total oocyte protein under these conditions was estimated to be ~84 h (Fig. 3 *A*), in good agreement with the previous estimate of ~73 h reported by Wallace and Hollinger (1979).

The chase of radiolabeled endogenous keratin from the soluble fraction was neither complete nor a simple logarithmic function of time (Fig. 3, *D* and *E*). Instead, an initial period of relatively rapid decline (estimated $t_{1/2}$ of ~3 h) was followed by a slower rate of decline (estimated $t_{1/2}$ of ~41 h). Overall, ~50–60% of the newly synthesized keratin was still present in the soluble fraction 16 h after methionine pool equilibration (Fig. 3 *E*). Radioactivity continued to accumulate as insoluble keratin throughout the chase; only a fraction of this increase could be accounted for by the movement of radioactive keratin from the soluble to the insoluble fraction (Fig. 3, *C* and *D*). The source of the additional radioactivity incorporated into insoluble keratin during the chase period is unclear. There are a number of polypeptides with very short half-lives in the oocyte (not shown), and it is possible that recycling of radioactive methionine may account for some of the continued incorporation of radioactivity into insoluble keratin.

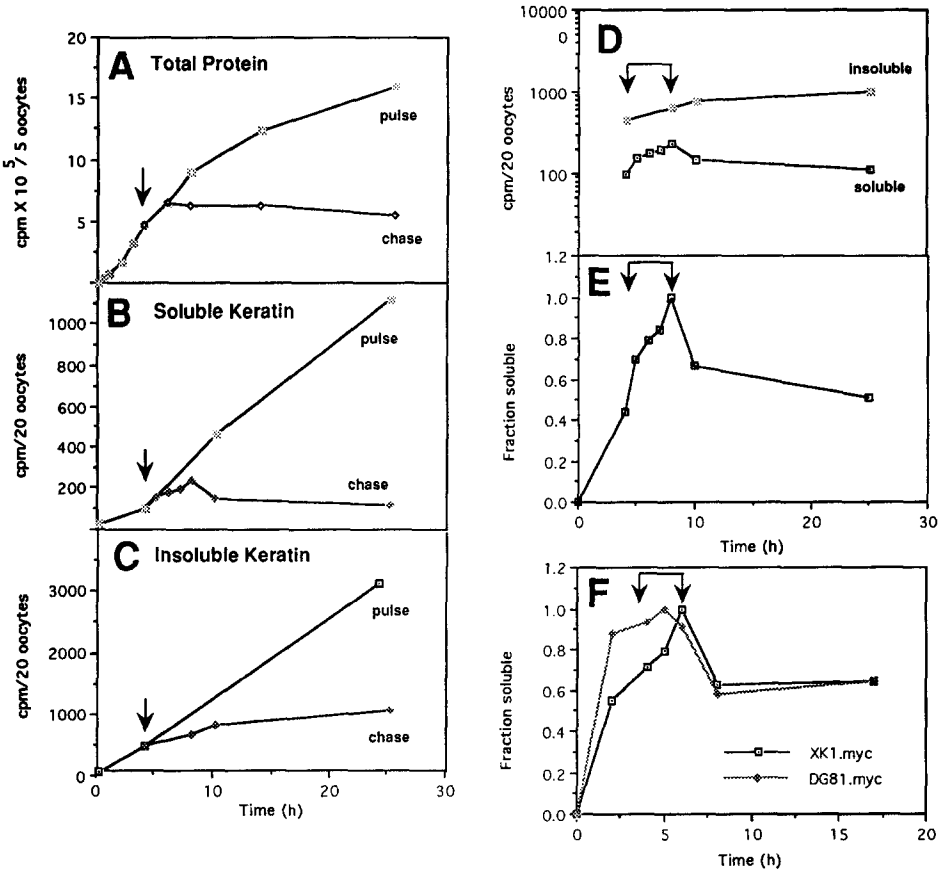

Figure 3. Keratin pulse-chase experiments. Uninjected (*A–E*) or keratin RNA-injected oocytes (*F*), were labeled with [^{35}S]methionine either continuously (*pulse*) or for 4 h followed by washing and subsequent incubation in medium containing unlabeled methionine (*chase*). For each time point the total TCA-precipitable radioactivity in triplicate sets of five oocytes was determined (*A*). Oocytes were partitioned into soluble (*B*) and insoluble (*C*) fractions, and the radioactivity associated with 1h5-reactive keratin (in the case of uninjected oocytes) or 9E10-reactive keratins (in the case of RNA-injected oocytes) was determined. In *B–E* each point represents the average of three sets of 20 oocytes per time point. The chase profile of both insoluble and soluble keratin from *B* and *C* is displayed on a semilogarithmic scale in *D* to compare distribution of labeled keratin between the two fractions during the chase. In *E* the fraction of the maximum amount of soluble endogenous keratin that accumulated during the pulse-chase experiment is displayed as a function of time. The chase profile of soluble endogenous keratin in *E* is similar to that observed for soluble XK1.myc and DG81.myc in analogous pulse-chase experiments with exogenous keratin (*F*). (*Arrows*, *A–C*) Beginning of chase; (*arrows*, *D–F*) duration of amino acid pool equilibration period.

To test whether the low overall rate of keratin synthesis was responsible for the failure to completely chase soluble keratin, we performed equivalent pulse-chase experiments using oocytes injected with RNAs encoding the XK1.myc and DG81.myc keratins. Despite the large increase in the overall rate of keratin synthesis seen in these oocytes (see Fig. 2 *D*), the pulse-chase characteristics of oocyte keratin were unchanged, with ~60% of the maximal amount of type I and type II soluble keratin synthesized during the pulse still occurring in the soluble fraction after an extended chase period (Fig. 3 *F*). Taken together, the simplest interpretation of these results is that keratin in the soluble fraction is not simply a posttranslational assembly intermediate, but rather represents a stable pool that can exchange with keratin in the insoluble fraction.

Forms of Soluble Keratin in the Oocyte

To examine the nature of the soluble keratin in the oocyte we used sucrose VGS and SEC. Previous VGS studies of cultured somatic cells had detected an ~7 S tetrameric species as the sole soluble form of IFP (Soellner et al., 1985; Franke et al., 1987; Chou et al., 1993). On the other hand, SEC has been used successfully to characterize monomer/dimer intermediates in the in vitro assembly keratin filaments (Coulombe and Fuchs, 1990). VGS analysis revealed a soluble ~7–8 S form of keratin in prophase *Xenopus* oocytes; the amount of this form increased upon oocyte maturation (Fig. 4) (see Klymkowsky et al., 1991).

Keratin tetramers are expected to migrate on SEC with an apparent molecular weight of 130,000–150,000 (Coulombe and Fuchs, 1990). When the soluble fraction of matured oocytes was analyzed by FPLC SEC, however, the majority of the soluble keratin eluted as a form with an apparent molecular weight of ~750,000 relative to globular protein molecular weight standards (Fig. 5 *A*). Similarly, when the soluble fraction of keratin RNA-injected oocytes was analyzed by SEC the majority of soluble myc-tagged keratin was present as an ~750-kD complex, together with a minor ~150-kD peak (Fig. 5, *B* and *C*). These results suggested that the majority of the soluble keratin in the oocyte is present in a form significantly larger than that predicted for a tetrameric complex, and that upon oocyte maturation, the keratin filament system of the oocyte is disassembled into the 750-kD keratin complex. This is consistent with our previous finding that the soluble keratin of matured oocytes behaves as an oligomeric complex (Klymkowsky et al., 1991; see *Discussion*).

Soluble Keratin in Reticulocyte Lysates

To further characterize the 750-kD keratin complex, we asked whether it was specific to the *Xenopus* oocyte or whether it could be formed in RRLs. RRLs efficiently

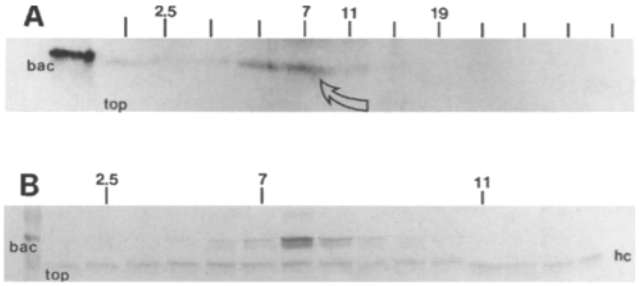

Figure 4. VGS analysis of soluble keratin in the oocyte. The soluble fraction of prophase (*A*) or matured (*B*) oocytes was fractionated on linear sucrose gradients. Gradient fractions were either precipitated with TCA and analyzed by SDS-PAGE and Western blotting using 1h5 (*A*), or were immunoprecipitated using the 1h5 antibody and then analyzed by SDS-PAGE and 1h5 Western blotting (*B*). A 1h5-reactive polypeptide (*open arrow*) cosedimented with a 7 S immunoglobulin standard in both prophase and M-phase oocytes (numbers above blot, sedimentation position of 2.5 S, 7 S, 11 S, and 19 S standards); the amount of the ~7 S keratin species was increased in matured oocytes. In *B*, the band migrating faster than the type II keratin is the immunoglobulin heavy chain (*hc*). *bac*, bacterially synthesized oocyte type II keratin included as a standard in both blots. *top*, top of gradients.

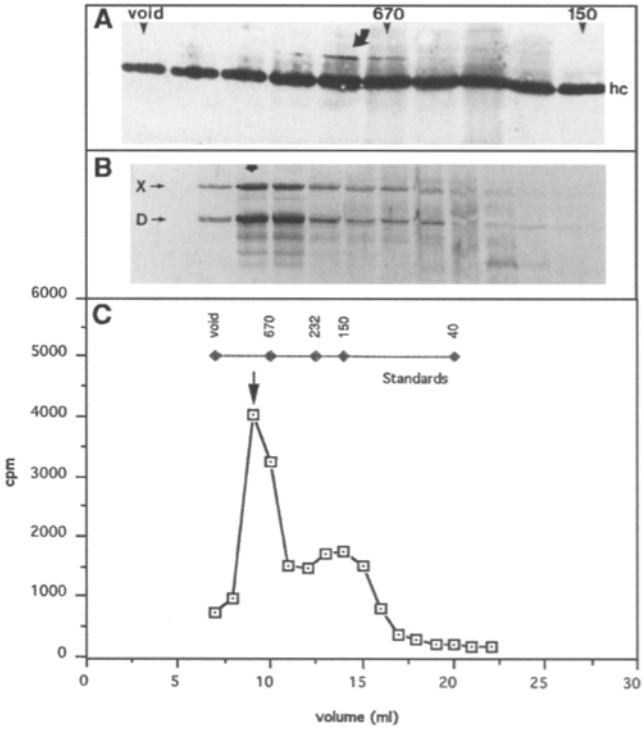

Figure 5. SEC analysis of soluble keratins in the oocyte. The soluble fractions of matured oocytes (*A*) or XK1.myc/DG81A.myc RNA-injected oocytes (*B*) were fractionated by SEC on either a Superose® 6 column (*A*) or a Superose® 12 column (*B*); each fraction was immunoprecipitated using either the 1h5 (*A*) or 9E10 (anti-myc) (*B*) antibodies. In both cases, the majority of soluble type II keratin was found in an ~750-kD form (*arrow*). In the case of the RNA-injected, [^{35}S]methionine-labeled oocytes, the amount of full-length XK1.myc polypeptide in each fraction was quantitated by excising the relevant bands and scintillation counting (*C*); the bulk of the soluble, exogenous XK1.myc migrated as an ~750-kD species, while a minor peak of radioactivity eluted with an apparent molecular weight of ~150,000. (*Arrows*, *B* and *C*) Peak XK1.myc fraction. (*Arrowheads*) Position of column's void volume (*void*) position of molecular weight markers of 670,000 and 150,000. *C*, elution positions of globular protein molecular weight standards used to calibrate the Superose® 12 column. *hc*, position of 1h5 heavy chain.

translate in vitro transcribed RNAs and preserve many aspects of native protein folding and assembly (see Lorimer et al., 1993). When RNAs encoding either the XK1.myc or the DG81A.myc polypeptides were translated individually, only an ~150-kD species was observed by SEC (Fig. 6, *A* and *B*). VGS analysis of such RRL reactions revealed a single peak that sedimented between 7 and 8 S (Fig. 7 *A*), as would be expected for a tetramer. When XK1.myc and DG81A.myc RNAs were cotranslated, however, SEC revealed a species migrating at 750 kD, together with a second form at ~135 kD (Fig. 6 *C*). Full-length XK1.myc and DG81.myc polypeptides cofractionated in the 750-kD peak while the 135-kD peak contained little, if any, full-length XK1.myc polypeptide (not shown, see Fig. 7 *B*). VGS analysis of RRL reactions synthesizing XK1.myc and DG81.myc together revealed a single form of keratin that sedimented between 7 and 8 S (Fig. 7 *A*). When type I and type II keratin complexes from RRL translation reactions were fractionated on higher percentage sucrose gradients capable of resolving complexes >19 S, the 7–8 S form of keratin was still the sole species observed (not shown). These results indicated that the keratin complexes generated in RRL behave similarly to those detected in the oocyte. In both systems an ~750-kD complex of type I and type II keratin was detected by SEC, whereas by VGS only an ~7–8 S species was detected.

These observations suggested that the 750-kD keratin complex might disassemble into a 150, 7 S form under the conditions of VGS. To examine the stability of the 750-kD complex, we examined the effects of prolonged dilution, as would occur during VGS analysis, on the behavior of the 750-kD keratin complex. When the 750-kD complex was rechromatographed immediately after isolation (by SEC), it refractionated as a 750-kD form (Fig. 7 *C*). On the other hand, when fractions containing the 750-kD keratin complex were incubated for 16 h on ice, a time period similar to VGS analysis, and then analyzed by SEC, a 150-kD keratin complex appeared (Fig. 7 *D*). Electrophoretic analysis indicated that the appearance of the 150-kD complex was not due to proteolysis of the keratins (Fig. 7, *B* and *D*). It therefore appears that the 750-kD keratin complex can reorganize to form a 7 S, 150-kD form during prolonged incubation. The sedimentation properties and the apparent molecular weight of the 150,000 species are consistent with those predicted for a tetrameric complex.

Urea Denaturation Studies of Keratin Complexes

Previous studies have shown that increasing concentrations of urea can be used to disassemble keratin filaments into their subunits (see Franke et al., 1983; Hatzfeld et al., 1985; Coulombe and Fuchs, 1990; Eichner and Kahn, 1990). On Superose® 12 columns, run under urea-denaturing conditions, keratin tetramers migrate with an apparent

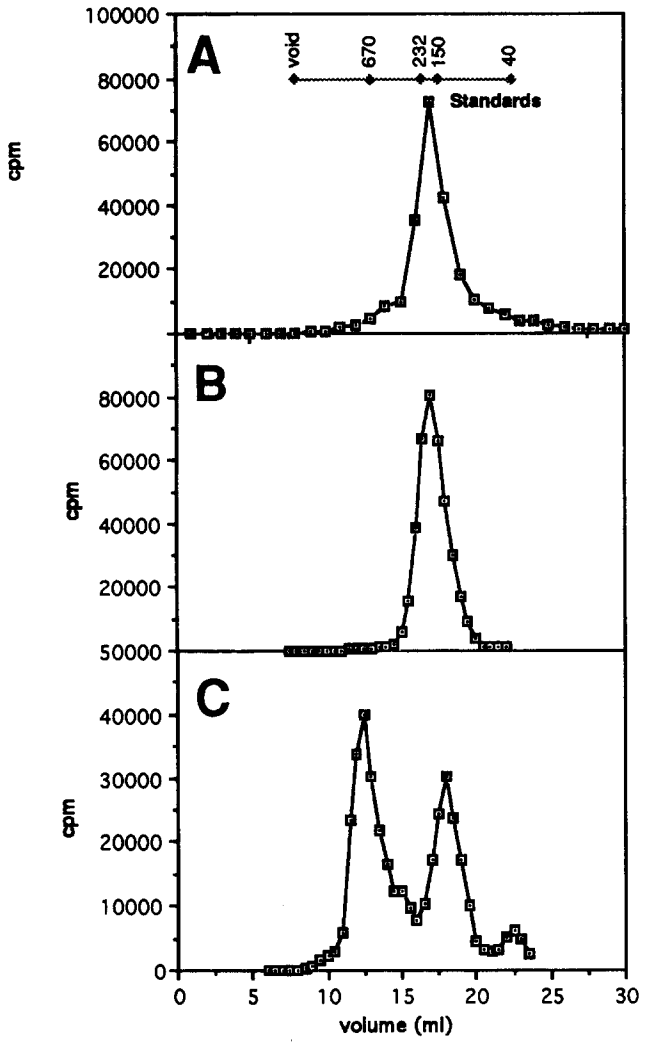

Figure 6. Forms of soluble keratin generated in RRL translation reactions. When the soluble fractions of RRL translation reactions synthesizing either XK1.myc (*A*) or DG81.myc (*B*) were analyzed by Superose® 6 SEC, a single ~150-kD species was observed. When RNAs encoding both XK1.myc and DG81.myc were cotranslated in RRL, however, a new ~750-kD species was detected by Superose® 6 SEC (*C*). *A* shows the elution position of protein molecular weight standards.

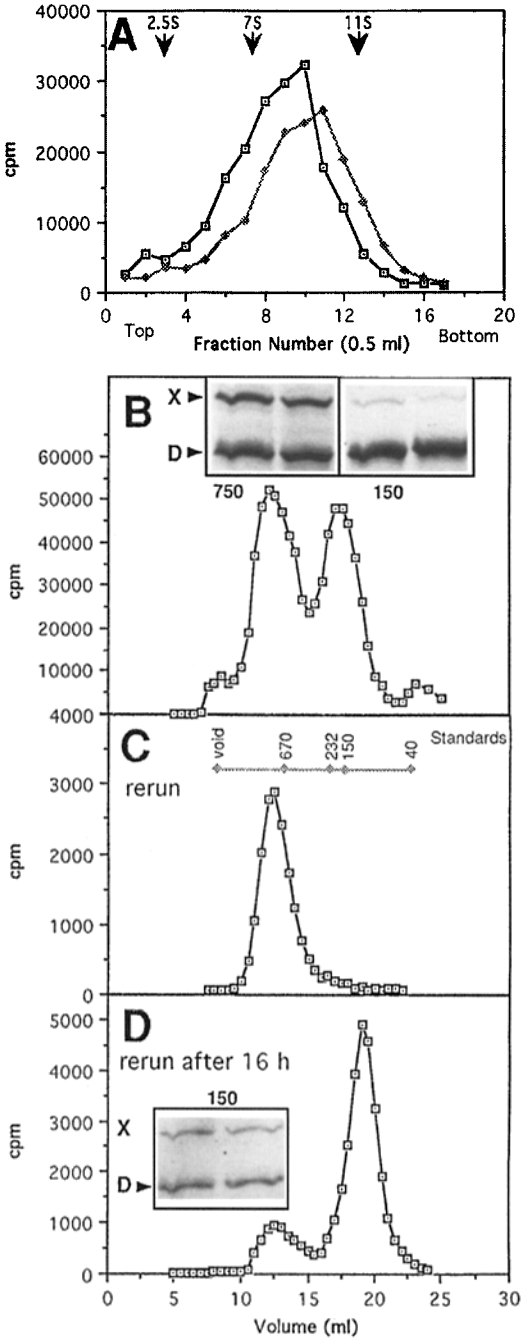

Figure 7. Stability of the 750-kD form of keratin. VGS analysis of either XK1.myc or XK1.myc/DG81.myc RRL cotranslation reactions revealed a single ~7–8 S species (*A*). To examine the stability of the 750-kD complex, Superose 6® SEC was used to isolate the 750-kD keratin complex from a XK1.myc/DG81.myc RRL cotranslation reaction (*B*). When rerun immediately on a Superose® 6 column, only the 750-kD form was observed (*C*); however, when the 750-kD keratin complex was incubated on ice for 16 h and then analyzed by Superose® 6 SEC, the majority of keratin migrated as an ~150-kD form (*D*). SDS-PAGE/autoradiography of the original 750- and 150-kD fractions (*B*, *inset*) revealed that the 750-kD peak contained roughly equal amounts of full-length XK1.myc (*X*) and DG81.myc (*D*) polypeptides, whereas the 150-kD peak contained relatively less full-length XK1.myc polypeptide. The 150-kD species formed after incubation of the 750-kD keratin complex on ice (*D*) reveals that its polypeptide composition is similar to the 750-kD keratin complex from which it was derived. *A*, top and bottom of the gradients, along with sedimentation positions of 2.5 S, 7 S, and 11 S standards. —⊡—, XK1; —◆—, XK1 + DG81.

molecular weight of ~135,000; monomers and dimers cofractionate with an apparent molecular weight of ~70,000–80,000 (Coulombe and Fuchs, 1990). Furthermore, at urea concentrations where keratin subunit interactions are maintained, type I and type II keratins focus together in the first dimension of two-dimensional gels due to their physical association in a complex. At higher urea concentrations the keratins dissociate and focus separately as monomers (Franke et al., 1983).

When aliquots from RRL XK1.myc and DG81.myc cotranslation reactions were equilibrated in 2 M urea and

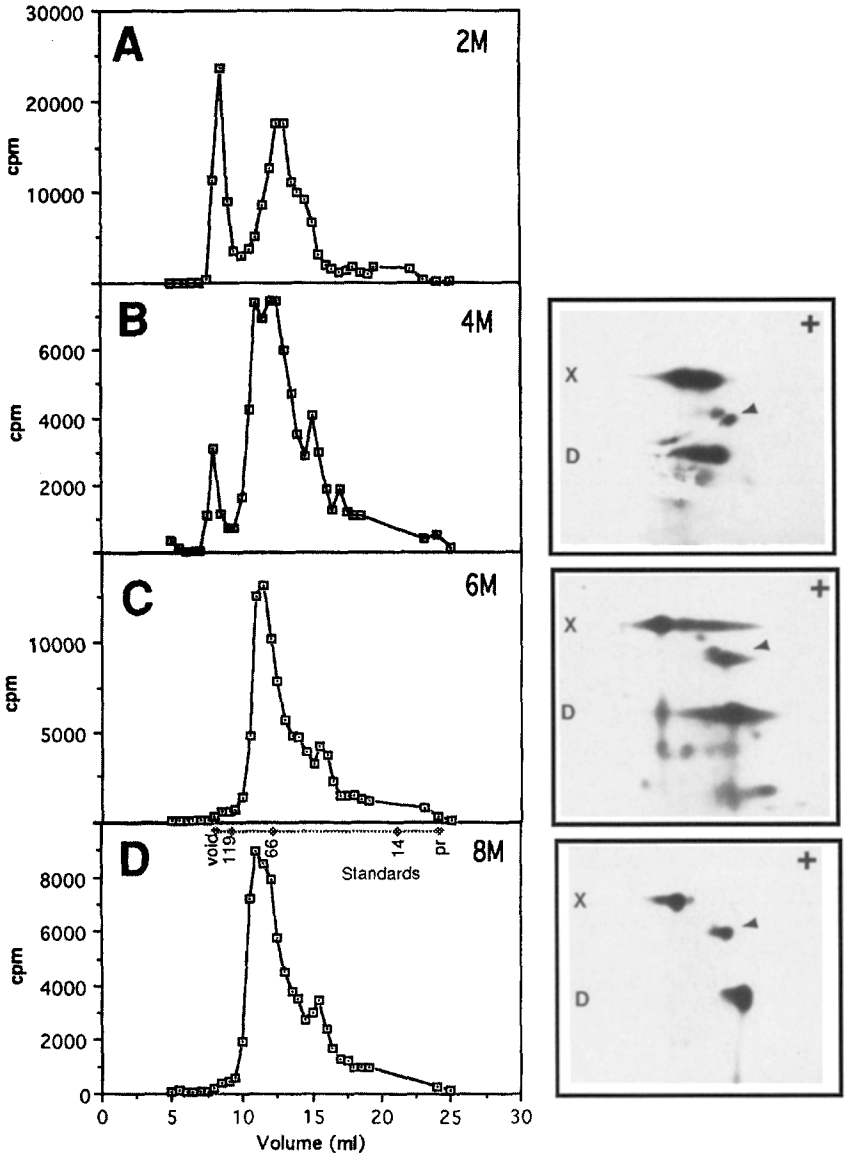

Figure 8. Urea denaturation analysis of RRL keratins complexes. RNAs encoding XK1.myc and DG81.myc were translated in RRL, and urea was added to final concentrations of 2, 4, 6, or 8 M. Samples were then fractionated using Superose® 12 SEC or analyzed by two-dimensional IEF-PAGE in the presence of 2, 4, 6, or 8 M urea (*A–D*). In 2 M urea, XK1.myc/DG81.myc fractionated as two species of ~130- and 80-kD (*A*). The amount of the 80-kD species seen by SEC increased with increasing urea concentration (*B–D*); in a corresponding manner, the degree to which the XK1.myc (*X*) and DG81.myc (*D*) keratins cofocused together in the IEF dimension of two-dimensional gels decreased with increasing urea concentration (*B–D*). *D*, position of protein molecular weight standards denatured in 8 M urea on Superose® 12 columns equilibrated in 8 M urea. +, acidic end of first-dimensional isoelectric focusing gels. The polypeptide migrating faster than XK1.myc in the second dimension (*arrowheads*) is the XK1.myc degradation product described in Fig. 1.

fractionated on Superose® 12 columns equilibrated in 2 M urea, the 750-kD species disappeared and the keratin migrated as ~130- and 80-kD species (Fig. 8 *A*; apparent molecular weights are based on the migration of molecular weight standards chromatographed in 8 M urea). As the urea concentration was increased to 4, 6, and 8 M, the relative amount of the 80-kD form increased until it was the sole form of keratin present in the reaction (Fig. 8, *B–D*).

Since apparent molecular weight values of molecular complexes on SEC are altered by the addition of urea, an important control in these experiments was to determine the urea denaturation behavior of XK1.myc alone. In the absence of urea, XK1.myc produced a single major peak of ~150,000 (see Fig. 6). In 2 M urea, RRL-translated XK1.myc resolved into two peaks with apparent molecular weights of ~130,000 and 80,000 (Fig. 9 *E*). This demonstrates that in the presence of urea, the 150-kD peak (observed under nondenaturing conditions) can give rise to both 130- and 80-kD species.

In 4 M urea, XK1.myc/DG81A.myc cotranslation RRL reactions behave as a single 80-kD species, as determined by SEC (run in the presence of 4 M urea). To determine if this species contained heterodimeric keratin, we analyzed the RRL reaction by two-dimensional gel electrophoresis under conditions in which the isoelectric focusing step was carried out in the presence of 4 M urea. Under these conditions, the keratins focused in a manner consistent with the presence of XK1.myc/DG81.myc heterodimers (see Fig. 8 *B*). As the urea concentration was increased, an increasing proportion of the XK1.myc and DG81.myc focused at their individual isoelectric points, although the keratins still fractionated as an ~80-kD form by SEC (Fig. 8, *C* and *D*). These results support the conclusion that the ~130–150-kD/7 S species is a tetramer that can be disassembled into dimers and eventually into monomers with increasing urea concentration (Franke et al., 1983; Coulombe and Fuchs, 1990). The 750-kD type I/II keratin complex, seen in both *Xenopus* oocytes and RRL reactions, is therefore a supratetrameric form of keratin; i.e., it is more than simply a keratin tetramer. Whether it is a higher order keratin oligomer, or a keratin tetramer complexed with some other factors, is not clear (see below).

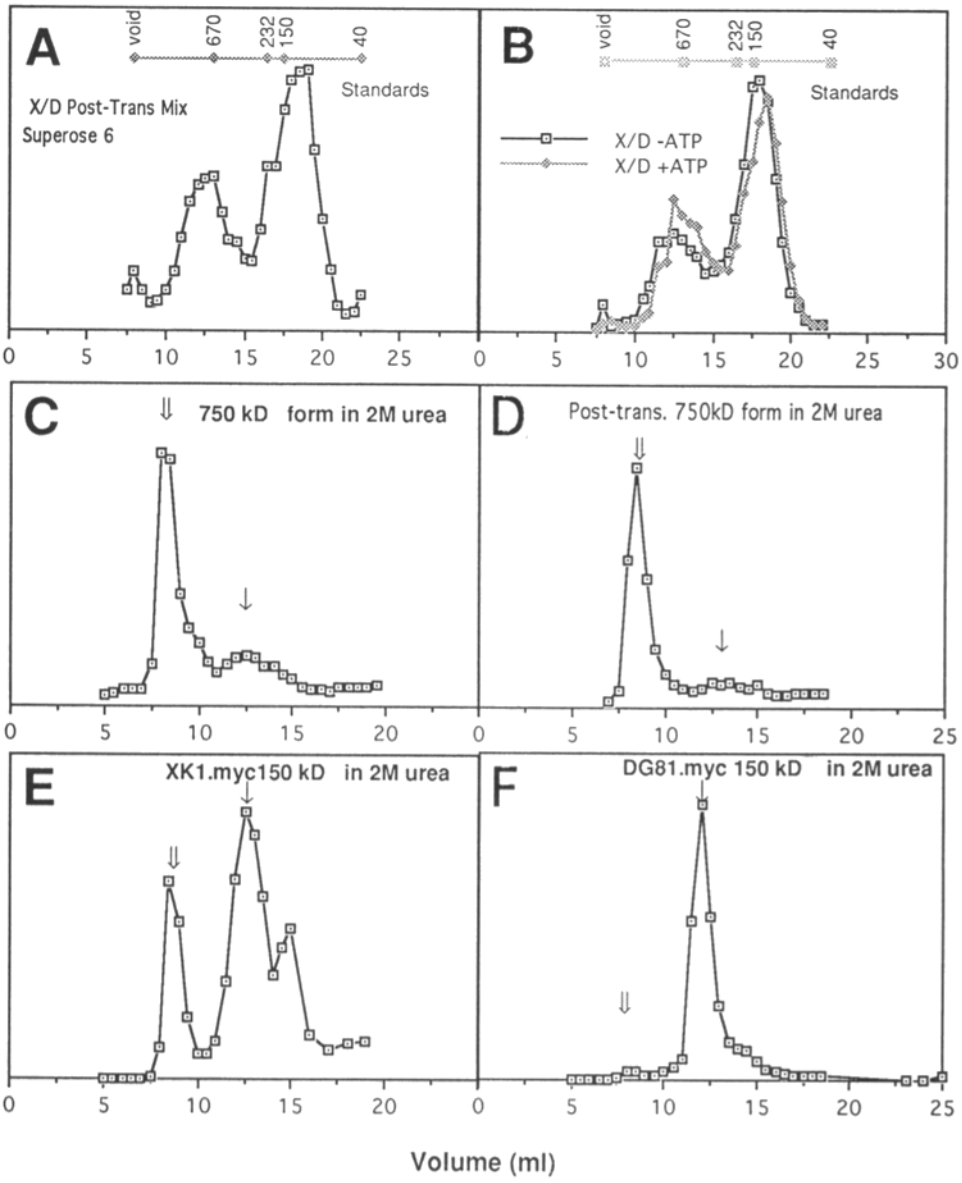

Figure 9. Posttranslation formation of the 750-kD keratin complex. XK1.myc and DG81.myc RRL translation reactions were treated with cyclohexamide and RNAse A to block further translation. The reactions were then mixed in a 1:1 ratio and incubated for 30 min at 30°C, followed by analysis by Superose® 6 SEC. Under these conditions, the 750-kD keratin complex was formed (*A*). To determine whether ATP hydrolysis was necessary for the posttranslational formation of the 750-kD keratin complex, aliquots of XK1.myc and DG81.myc RRL translation reactions were either treated with apyrase (20 U/ml) and 5 mM EDTA, to prevent further nucleotide hydrolysis, or were supplemented with 10 mM ATP/20 mM $MgCl_2$ and then combined, incubated at 30°C for 30 min, and then analyzed by Superose® 6 SEC (*B*). ATP levels had no apparent effect on 750-kD keratin complex formation. *A* and *B*, position of protein molecular weight standards on the Superose® 6 column. The stability of the posttranslationally formed 750-kD keratin complex was examined by treating incubation in 2 M urea; both posttranslationally formed (*C*) and cotranslationally formed (*D*) complexes dissociated into an ~130-kD species (*double-tailed arrow*); the 80-kD species (*single-tailed arrow*) was not observed. In contrast, the 150-kD XK1.myc and DG81.myc species used to generate the 750-kD keratin complex disassembled either partially (*E*, XK1.myc) or completely (*F*, DG81A) into the 80-kD species when treated with 2 M urea.

Posttranslational Formation of the 750-kD Keratin Complex

In our previous experiments, the 750-kD keratin complex was generated in RRL only when both type I and type II keratins were translated simultaneously. To determine whether the 750-kD complex could be formed posttranslationally, individual XK1.myc and DG81.myc RRL translation reactions were treated with cyclohexamide and RNAse A to block further translation. Equal volumes of the two reactions were mixed together at 30°C for 30 min and then analyzed by SEC. Under these conditions, the 750-kD keratin complex was formed, although not to the same extent as was typically observed in cotranslation reactions (Fig. 9 *A*). To determine whether ATP was necessary for the formation of the 750-kD keratin complex, individual XK1.myc and DG81A.myc translation reactions were treated with apyrase/EDTA or supplemented with Mg/ATP before mixing. The apyrase/EDTA treatment was successful in reducing ATP levels in the lysates to ~0.5 fmol/ml, as determined using a luciferase assay (not shown). However, the posttranslational formation of the 750-kD complex was not noticeably affected by the presence or absence of ATP (Fig. 9 *B*).

To determine whether posttranslationally assembled 750-kD keratin complex exhibited the same stability to urea denaturation as the form produced in cotranslation reactions, we examined its behavior in the presence of 2 M urea. Under these conditions, both posttranslationally (Fig. 9 *D*) and cotranslationally (Fig. 9 *C*) assembled 750-

kD keratin complex was converted into the 130-kD species. In contrast, when the 150-kD XK1.myc or DG81.myc species, used to form the 750-kD keratin complex, were analyzed in 2 M urea, XK1.myc produced both a 130-kD and an 80-kD form, while DG81A.myc produced only an 80-kD species (Fig. 9, *E* and *F*). These results suggest that posttranslational mixing of the type I and type II keratins results in the assembly of keratin heterodimers and heterodimeric tetramers which are more resistant to urea denaturation than the homomeric 150-kD species from which they were derived.

Discussion

A number of studies have demonstrated that an assembled IF is a dynamic structure, characterized by ongoing subunit exchange (see Heims and Aebi, 1994). Pulse-chase analysis of newly synthesized keratin in the *Xenopus* oocyte (Fig. 3) supports this conclusion. The chase kinetics observed for soluble and insoluble keratin in the prophase oocyte are essentially identical to those reported by Soellner et al. (1985) for vimentin in rat RVF-SMC cells. Soellner et al. (1985) interpreted their data in terms of a significant exchange reaction between soluble and insoluble, i.e., filamentous, forms of vimentin. Since increasing the overall rate of keratin synthesis by as much as 90-fold did not dramatically affect the chase kinetics of soluble keratin (Fig. 3), we conclude that the keratin exchange reaction must be substantially faster than the normal keratin synthesis rate in the oocyte.

A Novel Form of Soluble Keratin

Previous studies using VGS analysis had found that the major soluble form of IFP in cells is a 7–8 S, tetrameric species (Soellner et al., 1985; Franke et al., 1987; Chou et al., 1993) that then assembles into IFs (see Heims and Aebi, 1994). In our studies, we also found that the soluble keratin of prophase- and M-phase–arrested oocytes (Fig. 4) sedimented as a 7–8 S form. A similar 7–8 S species was found when RRLs were cotranslating XK1.myc/DG81.myc RNAs (Fig. 7 *A*). When soluble keratin was analyzed using SEC, however, the bulk of the intact keratin in both oocytes (Fig. 5) and RRL XK1.myc/DG81.myc cotranslation reactions (Fig. 6 *C*) migrated with an apparent molecular weight of ~750,000. The molecular weight of this form is distinctly different from the 130–150-kD tetrameric species previously described by Coulombe and Fuchs (1990). When RRL reactions translating XK1.myc or DG81.myc RNAs individually were analyzed by SEC, only a 150-kD complex, which sedimented at 7–8 S, was observed (Fig. 6, *A* and *B*). We have obtained similar results using vimentin RNA, which also generated only a 150-kD/7 S form (Bachant, 1993). These results raise the possibility that (*a*) keratin homotetramers form under RRL reaction conditions; (*b*) the 750-kD keratin complex is larger than tetramer; and (*c*) the formation of the 750-kD keratin complex requires the presence of both type I and type II keratins.

Electron microscopy of keratin tetramers formed in vitro show that they are elongated, rodlike structures (see Coulombe and Fuchs, 1990 and references therein) that do not migrate as a globular protein on SEC; monomers and dimers were found to comigrate with an apparent molecular weight of ~80,000, while tetramers migrated with an apparent molecular weight of 135,000–150,000. To confirm that the 750-kD keratin complex resolved by SEC was not just a keratin tetramer, we carried out both dilution and urea denaturation studies. When the 750-kD keratin complex was incubated for extended periods of time (~16 h) under dilute conditions, it disassembled, or was reorganized, into a 150-kD form (Fig. 7). The disassembly of the 750-kD keratin complex was not due to proteolytic degradation of the keratin polypeptides (Fig. 7) and so presumably represents a simple equilibrium reaction.

Urea denaturation analysis provides further evidence that the 750-kD keratin complex contains tetrameric keratin either as part of an oligomeric complex, or associated with nonkeratin polypeptides. Upon incubation with 2 M urea, the 750-kD complex disassembled (or rearranged) primarily into a 130-kD form (Figs. 8 *C* and 9 *C*). As the urea concentration was increased, an 80-kD form became the major species (Fig. 8). Under conditions where keratin migrated primarily as the 80-kD form by SEC, IEF analysis revealed that the type I and type II keratins remained as a presumably heterodimeric complex (Fig. 8). At higher urea concentrations the keratin still fractionated as an 80-kD form, but the type I and type II keratins were resolved as individual monomers by IEF. These results directly identify the 150/130-kD species as keratin tetramer and imply that the 750-kD keratin complex contains keratin tetramers, either as part of a higher order oligomer, or complexed with other factors.

Our studies indicate that the 150-kD species formed by DG81.myc, and to a lesser extent XK1.myc, are unstable under conditions of 2 M urea treatment and disassemble into an 80-kD form (Fig. 9, *E* and *F*). Furthermore, when RRL translation reactions of type I and type II keratins are mixed posttranslationally, a 750-kD keratin complex forms (Fig. 9 *A*). Urea denaturation analysis of this 750-kD keratin complex indicates that it contains tetramers (Fig. 9 *D*), and that these tetramers are similar in their stability to those formed in XK1.myc/DG81A.myc cotranslation reactions (Fig. 9 *C*). The ability of homodimers/homotetramers to reorganize into heterodimers/heterotetramers suggests the type of active keratin subunit exchange suggested by Miller et al. (1993) can occur within reticulocyte lysates and presumably also within the intact cell.

The lability of the 750-kD form also suggests a possible explanation for why it was not observed reproducibly in gradient sedimentation studies. Under the conditions of velocity sedimentation, the 750-kD keratin complex disassembles into the 130–150-kD form of keratin (Fig. 7). In a previous study, we found that the soluble keratin in the M-phase *Xenopus* oocyte sedimentated as a >11 S complex (Klymkowsky et al., 1991). When reexamined in the course of these studies, we found only a 7–8 S soluble form, suggesting that subtle differences in sedimentation conditions (which we have yet to identify) can stabilize (or destabilize) the larger oligomeric form of keratin.

It is worth noting that the apparent stability of *Xenopus* K8/K14 keratin tetramers to urea denaturation is lower in our system that was previously reported by Coulombe and Fuchs (1990) for human K5/K14 keratin tetramers. A

number of factors may account for this difference. First, these are *Xenopus* keratins, and the assembly of *Xenopus* IFP proteins has been found to differ in some significant ways from the behavior of their vertebrate homologues (see Herrmann et al., 1993). Second, the K8/K14 keratin pair used in our studies is an unnatural one; the normal partner of K8 would be either K18 or K19, while the normal partner of K14 would be K5 (see Fuchs and Weber, 1994). This could also influence tetramer and heterodimer stability. Finally, the presence of the myc-tagging epitope might influence tetramer/heterodimer stability. Nevertheless, the presence of the 750-kD keratin complex indicates that the major soluble form of keratin in the *Xenopus* oocyte and in RRLs translating both type I and type II keratins is not a simple tetramer (see below).

Speculation on the Nature of the 750-kD Keratin Complex

Chaperonin-like activities have been implicated in the biogenesis of both tubulins and actin (see Yaffe et al., 1992; Tian et al., 1995 and references therein). If a molecular chaperone were involved in keratin assembly, or in the suppression of keratin homodimer formation, the keratin–chaperone complex might be expected to have an apparent molecular weight on the order of 750,000. Several observations, however, argue against this possibility. First, the chaperone complexes characterized to date depend upon ATP to release their substrate proteins (Ellis and van der Vies, 1991; Lorimer et al., 1993). Yet, ATP has no apparent effect on the formation or stability of the 750-kD keratin complex (Fig. 9 *B*). Although the 750-kD keratin complex dissociates into tetrameric keratin under conditions of prolonged dilution (Fig. 7), pulse-chase studies revealed no obvious precursor/product relationship between the 750- and 150-kD forms in RRL translation reactions (not shown). In the case of tubulin, similar pulse-chase studies have shown that a high molecular weight complex containing tubulin polypeptides was a precursor to a smaller, assembly-competent form of tubulin (Yaffe et al., 1992).

It is possible that the 750-kD keratin complex represents an association of keratin dimers or tetramers with accessory factors present in the oocyte and in RRL. It has been reported that soluble keratins, extracted from liver cells, are associated with high molecular weight polypeptides (Sahyoun et al., 1982). In addition, there is a report that the 70-kD heat shock proteins can interact with keratins (Liao et al., 1995). We have examined immunoprecipitates of the type II keratin from late stage and matured *Xenopus* oocytes (Fig. 1), as well as from keratin RNA-injected oocytes (not shown) for accessory proteins; aside from the type I keratins, we find no other coprecipitated polypeptides associated with the keratins at stoichiometric levels. However, this analysis would not have detected unlabeled proteins, which may be stockpiled in the oocyte. In any case, we favor a model in which the 750-kD keratin complex is composed solely of keratin tetramers. We have yet to determine whether the 750-kD keratin complex is competent to assemble into filaments. Such an analysis is complicated by the apparent tendency of the 750-kD keratin complex to disassemble into tetramers (see above).

It has been proposed that IFP octamers are a structural unit of IFs (Aebi et al., 1983; Eichner et al., 1986; Hisanaga and Hirokawa, 1990; Geisler et al., 1992). Putative in vitro assembly intermediates of nonkeratin IFs, arrested at low ionic strength and visualized by electron microscopy, have been suggested to represent octameric forms of IFP (Ip et al., 1985; Hisanaga et al., 1990). VGS analysis of a putative NF-L octamer provided an apparent molecular weight of ~375,000 (Hisanaga et al., 1990). In the case of keratins, nucleation of keratin IF assembly has been proposed to require the formation of a six to eight keratin–polypeptide complex, and an octameric form appears to be one of a number of oligomeric species that forms during keratin filament assembly in vitro (Steinert, 1991). Although the true molecular weight of the 750,000 keratin complex is not known, it is possible that it is an octamer. Whatever its nature, however, the critical point is that the bulk of the soluble keratin, in both the prophase and the M-phase *Xenopus* oocyte, and in RRL reactions, is a 750-kD keratin complex, rather than a simple tetramer.

We thank Tom Sargent for the DG81A cDNA; Richard Guilfoyle and Shawn Christensen for their work in the isolation and characterization of the original XK1(8)b cDNA clone; Alberto Domingo, Joe Dent, Robert Cary, and Dave Shook for their help in the construction of various reagents; Karla Kirkegaard for access to her FPLC machine, and Mark Winey for entertaining our enthusiasm for this project.

This work was supported by grants from the National Science Foundation (89-0523) and the American Chemical Society (CB-71447). J. B. Bachant was supported by grants from the Colorado Institute for Biotechnology Research and a National Institutes of Health training grant appointment.

Received for publication 20 December 1993 and in revised form 5 October 1995.

References

Aebi, U., W. E. Fowler, P. Rew, and T. T. Sun. 1983. The fibrillar substructure of keratin filaments unraveled. *J. Cell Biol.* 97:1131–1143.

Bachant, J. B. 1993. Assembly and dynamics of keratin intermediate filaments in *Xenopus laevis* oocytes. Ph.D. Thesis, University of Colorado, Boulder.

Blikstad, I., and E. Lazarides. 1983. Vimentin filaments are assembled from a soluble precursor in avian erythroid cells. *J. Cell Biol.* 96:1803–1808.

Caplan, M. J., G. E. Palade, and J. D. Jamieson. 1986. Newly synthesized Na^+,K^+-ATPase α-subunit has no cytosolic intermediate in MDCK cells. *J. Biol. Chem.* 261:2860–2865.

Cary, R. B., and M. W. Klymkowsky. 1994. Differential organization of desmin and vimentin in muscle is due to differences in their head domains. *J. Cell Biol.*126:445–56.

Chou, C.-F., C. L. Riopel, L. S. Rott, and M. B. Omary. 1993. A significant soluble cytokeratin fraction in "simple" epithelial cells: role of phosphorylation and glycosylation. *J. Cell Sci.* 105:433–444.

Chu, D. T. W., and M. W. Klymkowsky. 1989. The appearance of acetylated α-tubulin during early development and cellular differentiation in *Xenopus*. *Dev. Biol.* 136:104–117.

Coleman, T. R., and E. Lazarides. 1992. Continuous growth of vimentin filaments in mouse fibroblasts. *J. Cell Sci.* 96:89–98.

Coulombe, P. A., and E. Fuchs. 1990. Elucidating the early stages of keratin filament assembly. *J. Cell Biol.* 111:153–169.

Dent, J. A., R. B. Cary, J. B. Bachant, A. Domingo, and M. W. Klymkowsky. 1992. Host cell factors controlling vimentin organization in the *Xenopus* oocyte. *J. Cell Biol.* 119:855–866.

Domingo, A., A. J. Sarria, R. M. Evans, and M. W. Klymkowsky. 1992. Studying intermediate filaments. *In* The Cytoskeleton: A Practical Approach. K. L. Carraway and C. A. C. Carraway, editors. Oxford University Press, New York. 223–255.

Eichner, R., and M. Kahn. 1990. Differential extraction of keratin subunits and filaments from normal human epidermis. *J. Cell Biol.* 110:1149–1158.

Eichner, R., T. T. Sun, and U. Aebi. 1986. The role of keratin subfamilies and keratin pairs in the formation of human epidermal intermediate filaments. *J. Cell Biol.* 102:1767–1777.

Ellis, R. J., and S. K. van der Vies. 1991. Molecular chaperones. *Annu. Rev. Biochem.* 60:321–347.

Evans, G. I., G. K. Lewis, G. Ramsay, and J. M. Bishop. 1985. Isolation of monoclonal antibodies specific for the human c-myc proto-oncogene product. *Mol. Cell. Biol.* 5:3610–3616.

Franke, W. W., D. L. Schiller, M. Hatzfeld, and S. Winter. 1983. Protein complexes of intermediate-sized filaments: melting of cytokeratin complexes in urea reveals different polypeptide separation characteristics. *Proc. Natl. Acad. Sci. USA.* 80:7113–7117.

Franke, W. W., S. Winter, E. Schmid, P. Söllner, G. Hammerling, and T. Achtstatter. 1987. Monoclonal cytokeratin antibody recognizing a heterotypic complex: immunological probing of conformational states of cytoskeletal proteins in filaments and in solution. *Exp. Cell Res.* 173:17–37.

Franz, J. K., and W. W. Franke. 1986. Cloning of cDNA and amino acid sequence of a cytokeratin expressed in oocytes of *Xenopus laevis*. *Proc. Natl. Acad. Sci. USA.* 83:6475–6479.

Franz, J. K., L. Gall, M. A. Williams, B. Picheral, and W. W. Franke. 1983. Intermediate-size filaments in a germ cell: Expression of cytokeratins in oocytes and eggs of the frog *Xenopus*. *Proc. Natl. Acad. Sci. USA.* 80:6254–6258.

Fuchs, E., and W. Weber. 1994. Intermediate filaments: structure, dynamics, function, and disease. *Annu. Rev. Biochem.* 63:345–382.

Gall, L., and E. Karsenti. 1987. Soluble cytokeratins in *Xenopus laevis* oocytes and eggs. *Biol. Cell (Paris).* 61:33–38.

Geisler, N., J. Schunemann, and K. Weber. 1992. Chemical cross-linking indicates a staggered and antiparallel protofilament of desmin intermediate filaments and characterizes one higher-level complex between protofilaments. *Eur. J. Biochem.* 206:841–852.

Gurdon, J. B., and M. P. Wickens. 1983. The use of *Xenopus* oocytes for the expression of cloned genes. *Methods Enzymol.* 101:370–386.

Hatzfeld, M., and W. W. Franke. 1985. Pair formation and promiscuity of cytokeratins: formation in vitro of heterotypic complexes and intermediate-sized filaments by homologous and heterologous recombinations of purified polypeptides. *J. Cell Biol.* 101:1826–1841.

Hatzfeld, M., and K. Weber. 1990. The coiled coil of in vitro assembled keratin filaments is a heterodimer of type I and II keratins: use of site-specific mutagenesis and recombinant protein expression. *J. Cell Biol.* 110:1199–1210.

Heims, S., and U. Aebi. 1994. Making heads and tails of intermediate filament assembly, dynamics and networks. *Curr. Opin. Cell Biol.* 6:25–33.

Herrmann, H., A. Eckelt, M. Brettel, C. Grund, and W. W. Franke. 1993. Temperature-sensitive intermediate filament assembly. Alternative structures of Xenopus laevis vimentin in vitro and in vivo. *J. Mol. Biol.* 234:99–113.

Hisanaga, S., and N. Hirokawa. 1990. Molecular architecture of the neurofilament. II. Reassembly process of neurofilament L protein *in vitro*. *J. Mol. Biol.* 211:871–882.

Hisanaga, S., A. Ikai, and N. Hirokawa. 1990. Molecular architecture of the neurofilament. I. Subunit arrangement of neurofilament L protein in the intermediate-sized filament. *J. Mol. Biol.* 211:857–869.

Ip, W., M. K. Hartzer, Y. Y. Pang, and R. M. Robson. 1985. Assembly of vimentin *in vitro* and its implications concerning the structure of intermediate filaments. *J. Mol. Biol.* 183:365–375.

Isaacs, W. B., R. K. Cook, A. J. Van, C. M. Redmond, and A. B. Fulton. 1989. Assembly of vimentin in cultured cells varies with cell type. *J. Biol. Chem.* 264:17953–17960.

Jonas, E., T. D. Sargent, and I. B. Dawid. 1985. Epidermal keratin gene expressed in embryos of *Xenopus laevis*. *Proc. Natl. Acad. Sci. USA.* 82:5413–5417.

Klymkowsky, M. W. 1995. Intermediate filament organization, reorganization, and function in the clawed frog *Xenopus*. *Curr. Top. Dev. Biol.* 31:455–486.

Klymkowsky, M. W., L. A. Maynell, and A. G. Polson. 1987. Polar asymmetry in the organization of the cortical cytokeratin system of *Xenopus laevis* oocytes and embryos. *Development (Camb.).* 100:543–557.

Klymkowsky, M. W., L. A. Maynell, and C. Nislow. 1991. Cytokeratin phosphorylation, cytokeratin filament severing, and the solubilization of the maternal mRNA Vg1. *J. Cell Biol.* 114:787–797.

Krieg, P. A., and D. A. Melton. 1984. Functional messenger RNAs are produced by SP6 *in vitro* transcription of cloned cDNAs. *Nucleic Acids Res.* 12: 7057–7070.

Liao, J., L. A. Lowthert, N. Ghori, and M. B. Omary. 1995. The 70-kDa heat shock proteins associate with glandular intermediate filaments in an ATP-dependent manner. *J. Biol. Chem.* 270:915–922.

Lorimer, G. H., M. J. Todd, and P. V. Viitanen. 1993. Chaperonins and protein folding: unity and disunity of mechanisms. *Philos. Trans. R. Soc. Lond. Ser. B Biol. Sci.* 339:297–303.

Miller, R. K., S. Khuon, and R. D. Goldman. 1993. Dynamics of keratin assembly: exogenous type I keratin rapidly associates with type II keratin in vivo. *J. Cell Biol.* 122:123–135.

Nishizawa, K., T. Yano, M. Shibata, S. Ando, S. Saga, T. Takahashi, and M. Inagaki. 1991. Specific localization of phosphointermediate filament protein in the constricted area of dividing cells. *J. Biol. Chem.* 266:3074–3079.

Okabe, S., H. Miyasaka, and N. Hirokawa. 1993. Dynamics of the neuronal intermediate filaments. *J. Cell Biol.* 121:375–386.

Pang, S. Y.-Y., A. Schermer, J. Yu, and T.-T. Sun. 1993. Suprabasal change and subsequent formation of disulfide-stabilized homo- and hetero-dimers of keratins during esophageal epithelial differentiation. *J. Cell Sci.* 104:727–740.

Sahyoun, N., P. Stenbuck, H. I. LeVine, D. Bronson, B. Moncharmont, C. Henderson, and P. Cuatrecasas. 1982. Formation and identification of cytoskeletal components from liver cytosolic precursors. *Proc. Natl. Acad. Sci. USA.* 79:7341–7345.

Skalli, O., and R. D. Goldman. 1991. Recent insights into the assembly, dynamics, and function of intermediate filament networks. *Cell Motil. Cytoskeleton.* 19:67–79.

Smith, M. H. 1970. Molecular weights of proteins and other materials including sedimentation, diffusion & frictional coefficients and partial specific volumes. *In* CRC Handbook of Biochemistry. H. A. Sorber, editor. Chemical Rubber Company, Cleveland, OH.

Soellner, P., R. A. Quinlan, and W. W. Franke. 1985. Identification of a distinct soluble subunit of an intermediate filament protein: tetrameric vimentin from living cells. *Proc. Natl. Acad. Sci. USA.* 82:7929–7933.

Steinert, P. M. 1990. The two-chain coiled-coil molecule of native epidermal keratin intermediate filaments is a type I-type II heterodimer. *J. Biol. Chem.* 265:8766–8774.

Steinert, P. M. 1991. Analysis of the mechanism of assembly of mouse keratin 1/keratin 10 intermediate filaments *in vitro* suggests that intermediate filaments are built from multiple oligomeric units rather than a unique tetrameric building block. *J. Struct. Biol.* 107:175–188.

Steinert, P. M., and R. K. Liem. 1990. Intermediate filament dynamics. *Cell.* 60: 521–523.

Studier, F. W., A. W. Rosenberg, J. J. Dunn, and K. W. Dubendorff. 1990. Use of T7 RNA polymerase to direct expression of cloned genes. *Methods Enzymol.* 185:60–89.

Tian, G., I. E. Vainberg, W. D. Tap, S. A. Lewis, and N. J. Cowan. 1995. Specificity in chaperonin-mediated protein folding. *Nature (Lond.).* 375:250–253.

Wallace, R. A., and T. G. Hollinger. 1979. Turnover of endogenous, microinjected & sequestered protein in *Xenopus* oocytes. *Exp. Cell Res.* 119:277–287.

Yaffe, M. B., G. W. Farr, D. Miklos, A. L. Horwich, M. L. Sternlicht, and H. Sternlicht. 1992. TCP1 complex is a molecular chaperone in tubulin biogenesis. *Nature (Lond.).* 358:245–248.